Chemical Engineering Science 83 (2012) 56–65

Contents lists available at SciVerse ScienceDirect

Chemical Engineering Science

journal homepage: www.elsevier.com/locate/ces

Quantitative dynamical relationships for the effect of rotation rate on frequency and waveform of electrochemical oscillations

Mónika Urvölgyi [a], Vilmos Gáspár [a], Timea Nagy [b], István Z. Kiss [b,*]

[a] Institute of Physical Chemistry, University of Debrecen, Egyetem tér 1, 4032 Debrecen, Hungary
[b] Department of Chemistry, Saint Louis University, 3501 Laclede Ave., St. Louis, MO 63103, USA

ARTICLE INFO

Article history:
Received 29 June 2011
Received in revised form
9 October 2011
Accepted 11 October 2011
Available online 11 November 2011

Keywords:
Electrochemistry
Nonlinear dynamics
Mathematical modeling
Model reduction
Oscillations
Nullclines

ABSTRACT

We investigate the effect of changing mass transfer conditions through variation of rotation rate of a rotating disk electrode on features of oscillatory dynamics of negative differential resistance electrochemical systems. The theoretical analysis and numerical simulation of a prototype two-variable electrochemical model show that for oscillations close to a Hopf bifurcation the frequency (ω) increases with increase in rotation rate (d) following an approximate square root formula $\omega \propto d^{1/2}$. For relaxation oscillations, the oscillations maxima, minima, and transition points between the high- and low-current states do not depend on rotation rate; the oscillation waveform invariance is explained using nullcline analysis by showing that the rotation does not affect the nullcline of the fast variable (electrode potential) along which the oscillations occur. The numerical and theoretical predictions are confirmed in experiments with copper electrodissolution in phosphoric acid electrolyte using a rotating electrode setup. The results thus indicate that simplifying concepts related to invariant manifolds and parameter dependence of bifurcation points (principle of critical simplification) are efficient approaches to obtaining quantitative dynamical relationships for decoding complexity in electrochemical reaction systems.

1. Introduction

Efficient design of chemical reactors often requires theoretical treatment of complex chemical systems in which the dynamics is strongly influenced by emergent effects of principles of thermodynamics, reaction kinetics, and mass and heat transfer (Newman, 1968). Simplifying concepts greatly enhance the success of mathematical tools (e.g., those of nonlinear dynamics) for decoding the dynamical complexity (Epstein and Pojman, 1998). General, reliable mathematical techniques have been developed (Gorban et al., 2007) with which description of systems of many degrees of freedom is possible with only a few variables. Major directions with remarkably different approaches include the use of invariant manifolds (Bykov et al., 2008; Gorban and Karlin, 2003, 2005; Roussel and Fraser, 2001), coarse graining dynamics (Bindal et al., 2006; Kevrekidis et al., 2004; Theodoropoulos et al., 2000), and principle of critical simplification (Yablonsky et al., 2003). Location of invariant manifolds can greatly enhance description of nonlinear systems which are strongly influenced by the presence of small parameters (Strogatz, 2000). For example, nullcline techniques have been used for interpretation of relaxation oscillation in chemical reacting systems by identification of fast and slow variables and their distinct dynamics; in these examples, the small parameter is the ratio of the typical timescales of the fast and slow variables (Gáspár et al., 1991; Scott, 1994). The 'principle of critical simplification' (PCS) aims to describe the system by competing processes near bifurcation points without isolation of limiting steps typically used in classical quasi-stationary treatments (Yablonsky et al., 2003). An application of PCS, which is a combination of bifurcation theory and singular perturbation, resulted in relatively simple rate equations of catalytic CO oxidation at the saddle-node bifurcation point. The simplifying concepts thus often fill the gap between the relatively simple experimental results on dynamical behavior and parametric dependence of self-organized critical behavior and the complicated, multi-scale theoretical description of the systems that applies combination of strongly nonlinear ordinary and partial differential equations.

Electrochemical systems provide excellent examples where multi-scale modeling of charge-transfer chemical reactions, distribution of charged substances in the electrical double-layer, potential and current distribution in the electrolyte, and diffusion and convection of the electrolyte are required to describe the behavior of galvanic or electrolytic cells (Boovaragavan et al., 2009; Newman and Thomas-Alyea, 2004). Nonetheless, low-dimensional models that use electrode potential and near surface and Nernst diffusional layer concentrations

* Corresponding author. Tel.: +1 314 977 2139; fax: +1 314 2521.
E-mail address: izkiss@slu.edu (I.Z. Kiss).

0009-2509/$ - see front matter © 2011 Elsevier Ltd. All rights reserved.
doi:10.1016/j.ces.2011.10.073

of substances have proved to be sufficient in interpreting saddle-node, Hopf, homoclinic, and period-doubling bifurcations in bistable and oscillatory dynamics (Hudson and Tsotsis, 1994; Kiss et al., 2011; Koper, 1996; Krischer, 1999; Krischer and Varela, 2003; Plenge et al., 2003). Because of the time-scale separation of the electrode potential (fast variable due to fast double-layer charging) and the concentration of substances (slow variables), nullcline techniques have been successfully applied to interpret the existence of oscillations and multistationary behavior (Koper, 1996; Krischer, 1999; Toni et al., 1998). In large majority of electrochemical systems, the rate of reaction (expressed as Faradayic current) exhibits negative differential resistance (NDR) in a certain region of the overpotential; this negative differential resistance is the major source for oscillations and bistability (Strasser et al., 1999).

There exist a few skeleton models for NDR systems that can give proper qualitative picture of the bifurcation structure in wide class of electrochemical systems (Krischer, 1999; Strasser et al., 1999). Using such a simple model, we have derived and experimentally verified a scaling relationship for the dependence of Hopf bifurcation points on electrode surface area and rotation rate of the electrode that affects the mass transfer of electroactive species through changes in the thickness of the Nernst diffusion layer (Kiss et al., 2009a). Similarly, a simple frequency formula was derived that approximated the frequency of the oscillations in the Hopf bifurcation point as the inverse geometric mean of the electrical (double layer charging, capacitance x cell resistance) and chemical (Nernst diffusion layer thickness/rate constant) time-scales of the system (Kiss et al., 2009b). The theoretically predicted dependence of oscillation frequency on cell resistance has been experimentally confirmed in Cu electrodissolution (Kiss et al., 2009b).

In this paper, we investigate the effect of rotation rate on oscillatory dynamics of negative differential resistance electrochemical systems. For electrochemical systems with unique stable steady-state under mass transfer control the current, i, depends on the square root of the rotation rate (d) according to the classical Levich equation, $i \propto d^{1/2}$ (Bard and Faulkner, 1980; Levich, 1962). Here, we study quantitative dynamical relationships related to rotation rate dependence of strongly nonlinear oscillatory electrochemical systems for which mass transfer control plays an important role. For oscillations close to Hopf bifurcation, we derive a relatively simple equation for the frequency dependence on rotation rate by combining the previously obtained frequency formula (Kiss et al., 2009b) and rotation rate dependence of bifurcation points (Kiss et al., 2009a). For relaxation oscillations (that occur farther away from Hopf bifurcation), the waveform (maximum and minimum, and other characteristic points) of oscillations is analyzed as a function of the rotation rate using nullcline technique. The numerical and theoretical results obtained with a prototype two-variable model are verified in an experimental system: Cu electrodissolution in phosphoric acid. We have chosen Cu electrodissolution because the reaction has high level of reproducibility (Kiss et al., 2009a, 2009b) and the dynamical features have been well characterized (Albahadily et al., 1989; Albahadily and Schell, 1988; Glarum and Marshall, 1985; Schell and Albahadily, 1989); for example, it was shown that the amplitude exhibits a square root dependence on distance from the bifurcation point as the circuit potential is increased. (Albahadily and Schell, 1988) Finally, we discuss the agreement between experimental and numerical results, the relationships to the classical Levich equation, and the generality of the findings.

2. Material and methods

Experiments were performed by using a standard three-electrode electrochemical cell equipped with a 5 mm diameter copper rotating disk electrode (RDE), a Pt-sheet counter electrode, and a Hg/Hg_2SO_4/saturated K_2SO_4 or saturated calomel reference electrode. A potentiostat (Elektroflex EF451 or Pine AFCBP1) was applied to set the potential (resolution 0.01 mV) between the working and reference electrodes. All potentials are given with respect to Hg/Hg_2SO_4/saturated K_2SO_4 electrode. The current was measured with the ammeter built in the potentiostat. The sampling frequency for data acquisition was 200 Hz. The temperature of the cell was maintained with a circulating bath at the given values (-5, 5, or 10 °C) $\pm$ 0.1 °C. The electrolyte was 85% ortho-phosphoric acid. The surface of the copper electrode (99.99% purity) was wet polished by a series of sandpapers (P180–P4000). Before experiments cyclic polarization curves were obtained between -150 and 500 mV to ensure that previously observed behavior (Kiss et al., 1998) is reproduced. After this electrode pretreatment, the uncompensated series resistance was measured with impedance spectroscopy (Bard and Faulkner, 1980; Kiss et al., 1998), which was found to be $R_u = 35 \pm 5\ \Omega$. The working electrode was connected to the potentiostat through an external resistance R_{ext}; the total resistance R of the cell is the sum of the external resistance R_{ext} and the uncompensated series resistance R_u. With the experimental results we always give and discuss the total resistance R. Additional experimental procedures (e.g., electrode pretreatments and polarization curves) are described in previous publications (Kiss et al., 1997, 1998, 2009a). The frequencies of the current oscillations were determined as the inverse of the mean peak-to-peak periods.

Numerical tools: the ordinary differential equations were solved numerically with XPPAUT program package (Ermentrout, 2002) applying a Gear method with absolute error limit of 10^{-6}.

3. Results

3.1. Theory and simulation

3.1.1. Effect of rotation rate on frequency of electrochemical oscillators close to Hopf bifurcation theory

Previous quantitative relationships (Kiss et al., 2009a, 2009b) about the dynamics of a potentiostatic N-NDR type electrochemical oscillator were derived using a prototype model (Koper and Sluyters, 1991)

$$C_d \frac{de}{dt} = \frac{V-e}{AR} - nFk(e)c \tag{1}$$

$$\frac{dc}{dt} = -\frac{2}{a}k(e)c + \frac{2D}{a^2}(c_0 - c) \tag{2}$$

The equations utilize charge balance (Eq. (1)) and mass balance (Eq. (2)) to describe the behavior of essential variables: the electrode potential e and near-surface concentration of the electroactive species, c. Model parameters are the surface area (A) and the double layer capacitance per surface area (C_d) of the electrode; the number of electrons in the reaction (n), circuit potential (V), total series resistance (R), Nernst diffusion layer thickness (a); D and c_0 are the diffusion constant and the bulk concentration of the electroactive species, respectively. F is the Faraday constant. k(e) is the potential dependent rate constant; for NDR systems in this study $k(e)$ exhibits N-shaped dependence on e with a negative differential resistance region. (Koper, 1996; Krischer, 1999) The experimentally observable quantity, the current is obtained as $i(t) = (V - e(t))/R$.

The frequency of the oscillator was analyzed at a Hopf bifurcation point, and it was found that an approximation (upper limit) of the frequency (in unit of Hz) can be given as (Kiss et al.,

2009b)

$$\omega = \frac{1}{2\pi}\sqrt{\frac{2k(e_H)}{aC_dRA}} \tag{3}$$

where e_H is the electrode potential at the bifurcation point. Note that the simplicity of the equation lies in the use of e_H that depends in a complicated manner on system parameters (most importantly, V and R). By noting that the electrical (τ_{el}) and chemical (τ_{chem}) time scales in the system can be identified as

$$\tau_{el} = C_dAR \quad \text{and} \quad \tau_{chem} = \frac{a}{2k} \tag{4}$$

we can also express the frequency with the inverse of the geometric mean of the electrical and chemical time-scales

$$\omega = \frac{1}{2\pi}\sqrt{\frac{1}{\tau_{chem}\tau_{el}}} \tag{5}$$

Note that in electrochemical systems typically $\tau_{el} \ll \tau_{chem}$, because charging the double layer is a fast process compared to the slower chemical reactions (Bard and Faulkner, 1980).

Here, we consider the dependence of frequency on rotation rate (d) that affects only the Nernst diffusion layer thickness a in Eq. (3) through the well known Levich formula (Bard and Faulkner, 1980)

$$a = 1.61D^{1/3}\nu^{1/6}d^{-1/2} \tag{6}$$

where ν is the kinematic viscosity. The expression of a in Eq. (6) can be substituted into Eq. (3) to give the frequency at the bifurcation point

$$\omega = \frac{d^{1/4}}{2\pi}\sqrt{\frac{2k(e_H)}{1.61D^{1/3}\nu^{1/6}C_dRA}} \tag{7}$$

However, as the rotation rate is changed, the position of the Hopf bifurcation point, and thus e_H is changed. A convenient experimental procedure could include a primary change of rotation rate after which the total cell resistance (R) is adjusted such that the bifurcation point (with changes in circuit potential V) occurs at the same e_H value. Therefore, we can rearrange Eq. (7) as

$$\omega^2 R = d^{1/2}\frac{2k(e_H)}{1.61D^{1/3}\nu^{1/6}C_dA4\pi^2} \tag{8}$$

or

$$\omega^2 R \propto d^{1/2} \tag{9}$$

Therefore, a plot of $\omega^2 R$ vs. $d^{1/2}$ should give a straight line that starts from the origin.

In a previous publication (Kiss et al., 2009a), we have shown that at the Hopf bifurcation point

$$RA - C^* = \frac{D^*}{\sqrt{d}} \tag{10}$$

where C^* and D^* are constants that depend on e_H, D, c_0, n, and F. Using Eq. (10) for the R value in Eq. (9) yields

$$\omega^2 \propto \frac{\sqrt{d}}{C^* + (D^*/\sqrt{d})} \tag{11}$$

For typical oscillatory conditions C^* is smaller than RA (Kiss et al., 2009a); therefore, for relatively large external resistances $RA \approx D^*/\sqrt{d}$; this equation can be substituted in Eq. (9) to give

$$\omega \propto \sqrt{d} \tag{12}$$

Eq. (12) thus predicts that the frequency of the oscillations at the bifurcation point could exhibit an approximate square root dependency on rotation rate when the Hopf potential e_H is kept constant by adjustments of total external resistance R and circuit potential V. Conversely, when the relationship predicted by Eq. (12) is recovered in an experiment, it is an indication that the major assumption $C^* \ll RA$ holds for the system. Note that the existence of simple square root dependence of frequency on rotation rate is strongly nontrivial and thus requires confirmation in numerical simulations because of the assumptions used in the derivation.

3.1.2. Effect of rotation rate on frequency of electrochemical oscillators close to Hopf bifurcation: simulation

Next we carry out numerical simulations to confirm the rotation rate dependence of frequency (Eqs. (9) and (12)) in the Koper–Gaspard model (Koper and Gaspard, 1992) reduced to two-variables (Kiss et al., 2009a)

$$\epsilon\frac{d\bar{e}}{d\bar{t}} = \frac{\bar{v}-\bar{e}}{\bar{r}} - 120\bar{k}(\bar{e})\bar{c} \tag{13}$$

$$\frac{d\bar{c}}{d\bar{t}} = -1.25\sqrt{\bar{d}}\,\bar{k}(\bar{e})\bar{c} + \frac{4}{3}\bar{d}(1-\bar{c}) \tag{14}$$

where we use bar to denote dimensionless quantities that formally correspond to the actual physical quantities in Section 3.1.1. (ϵ is a time-scale parameter that corresponds to the double layer capacitance). The potential dependent rate constant is defined as

$$\bar{k}(\bar{e}) = 2.5\bar{\theta}^2 + 0.01\exp[0.5(\bar{e}-30)] \tag{15}$$

where $\bar{\theta}$ is related to the potential dependent surface coverage by the electroactive species

$$\bar{\theta} = \begin{cases} 1 & \text{for} \quad \bar{e} \le 35 \\ \exp[-0.5(\bar{e}-35)^2] & \text{for} \quad \bar{e} > 35 \end{cases} \tag{16}$$

Fig. 1a shows a typical, oscillatory current with a frequency of $\omega = 0.80$ at $\epsilon = 1$, $\bar{r} = 0.035$, and $\bar{d} = 0.115$; the applied circuit potential $\bar{v} = 36.752$ was determined in such a way that it is just above (by 0.001 increment) the Hopf-bifurcation point. The mean value of the electrode potential oscillations approximate the Hopf potential $\bar{e}_H = 35.448$. The obtained frequency value can be interpreted using the frequency formula (Eqs. (3) and (5)): the electrical timescale in Eq. (13) is $\bar{\tau}_{el} = \epsilon\bar{r} = 0.035$, the chemical timescale in Eq. (14) is

$$\bar{\tau}_{chem} = 1/\left[1.25\sqrt{\bar{d}}\,\bar{k}(35.448)\right] = 1.0734$$

giving a frequency estimate using Eq. (5) as 0.82. The ~3% overestimate comes from neglecting the diffusional time-scale contributions to the frequency (Kiss et al., 2009b). Note that the ratio of the electrical and chemical timescales $\bar{\tau}_{el}/\bar{\tau}_{chem} = 0.0326$ could be considered as small parameter often needed for strongly nonlinear response.

To promote the use of the frequency equation, we propose a simple potential step numerical experiment with which the chemical time-scale of the reaction can be approximated. When at low resistance value ($\bar{r} \to 0$), the potential is stepped to a value that corresponds to a Hopf potential, a transient current response can be measured as shown in Fig. 1b. Because the electrical time-scale is short (in the example it is 0.035) we shall see a decaying current, which is governed by the equation for the near-surface concentration of the chemical species. Diffusion is often a slow process, therefore, the time-scale of the decay can be associated with the time-scale of the chemical reaction. In Fig. 1c, the inverse slope of the semilogarithmic plot corresponding to the exponential decay of the current gives the chemical time-scale as 0.91. The frequency using this time-scale would be 0.89 which approximates well the numerically found value (0.80).

In the following, we test the effect of rotation rate on the frequency. Numerical simulations were performed for rotation

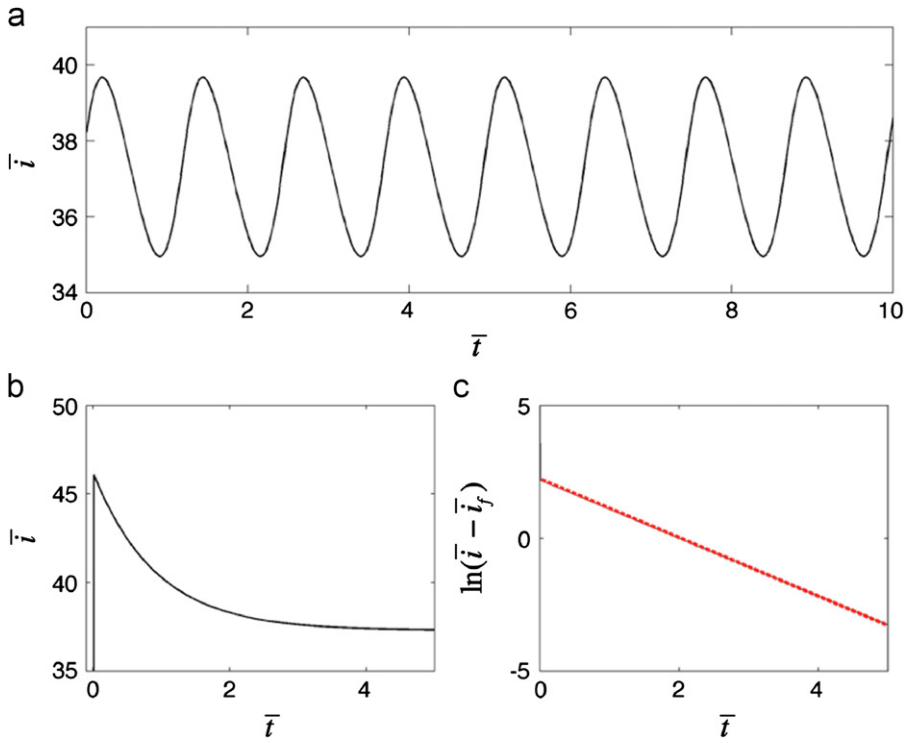

Fig. 1. *Simulations*: smooth periodic current oscillations close to Hopf bifurcation (top) and determination of chemical time-scale using step chronoamperometry (bottom) in a prototype model for negative-differential-resistance electrochemical system (Eqs. (13) and (14)) at rotation rate $\bar{d}=0.115$ and $\epsilon=1$. (a) Time series of current oscillations with frequency of $\omega=0.80$ Hz at $\bar{r}=0.035$, $\bar{v}=36.752$; (b) potential step response with nearly strictly potentiostatic cell control ($\bar{r}=1\times10^{-4}$). At $t=0$ the circuit potential was changed from $\bar{v}=35.7$ to 35.448; and (c) semilogarithmic plot for the exponential decay shown in panel b. The slope of the fitted line is -1.10. ($\bar{i}_f=37.288$ is the steady-state current value in panel b at $\bar{v}=35.448$).

rate ranging from 0.0575 to 0.92. For each rotation rate, the resistance and circuit potential were adjusted in such a way that at the Hopf bifurcation point the electrode potential was set to $\bar{e}_H=35.448\pm0.003$ and the mean current and the frequency of the oscillations were recorded. As it is shown in Fig. 2, the mean current exhibits nearly square root dependence ($\langle\bar{i}\rangle\propto\bar{d}^{0.40}$) and the resistance needed for oscillations decreases with increasing the rotation rate close to the expected inverse square root dependency $\langle\bar{r}\rangle\propto\bar{d}^{-0.39}$. More importantly, the $\omega^2\bar{r}$ quantity exhibits linear dependence on $\sqrt{\bar{d}}$ and the dependence of frequency on rotation rate is very close to the expected square root equation ($\omega\propto\bar{d}^{0.45}$).

The numerical simulations thus confirm that the frequency of the oscillations, under the constraint of constant Hopf potential and close to the Hopf bifurcation point, exhibits square root dependence on rotation rate in a simple electrochemical model for negative differential resistance electrochemical systems.

3.1.3. *Effect of rotation rate on oscillation waveform for relaxation oscillators*

The model Eqs. (13) and (14) can also exhibit classical relaxation oscillations when the timescale parameter ϵ in Eq. (13) is decreased to 0.1. (This decrease is necessary to further decrease the ratio of electrical and chemical timescales and thus provide a possibility for the existence of slow invariant manifolds.) The oscillations still arise through a supercritical Hopf bifurcation with smooth waveform as the circuit potential is increased; however, the oscillations slow down and develop strongly nonlinear waveform farther away from bifurcation point as shown in Fig. 3. Analytical derivations for oscillation waveform and amplitude for the region of potentials when the smooth oscillations close to Hopf bifurcation are transformed to relaxation oscillators is troublesome, however, some generalities can be observed about the effect of rotation rate on oscillations with strong relaxation character.

The relaxation oscillations are shown at fixed circuit potential for various rotation rates in the range of $\bar{d}=0.2$–0.8 in Fig. 3. Note that in contrast to oscillations in the Hopf region, we compare the behavior at fixed circuit potential instead of the Hopf potential. Therefore, the oscillations correspond to changing a single parameter. The relaxation oscillations consist of periods where, starting from current minimum, the current slowly increases, abruptly jumps to a high value, slowly decreases, and abruptly jumps to a low value to reach the minimum again.

Close inspection of oscillation waveform (see Fig. 4a) reveals a peculiar character of the waveform. The maximum, minimum, and the transition points (quick jumps between the high and low current states) occur at exactly the same current level at the different rotation rates. Although there are significant changes in the waveform of the current, these points remain unchanged during the oscillatory cycle. The mean current of the oscillations, shown in Fig. 4b, does follow the Levich equation (Bard and Faulkner, 1980): it increases with rotation rate in a nearly square root manner ($\langle\bar{i}\rangle\propto\bar{d}^{0.53}$). This increase is established by keeping the maxima, minima, and the transition points of the oscillations at constant level. As it is shown in the oscillatory waveform (Fig. 3a), at low rotation rate, the current stays low for large period of the cycle and quickly returns. At large rotation rate (Fig. 3d), the current stays at the high level stage for long period to where it returns after a quick excursion to the low current state. The mathematical explanation for establishment of Levich equation for the mean current during the oscillation is very difficult.

The invariant maxima and minima of the oscillations and the transition points can be interpreted using a nullcline technique. The $\bar{e}$ variable is considered fast, therefore, the variations of $\bar{e}$

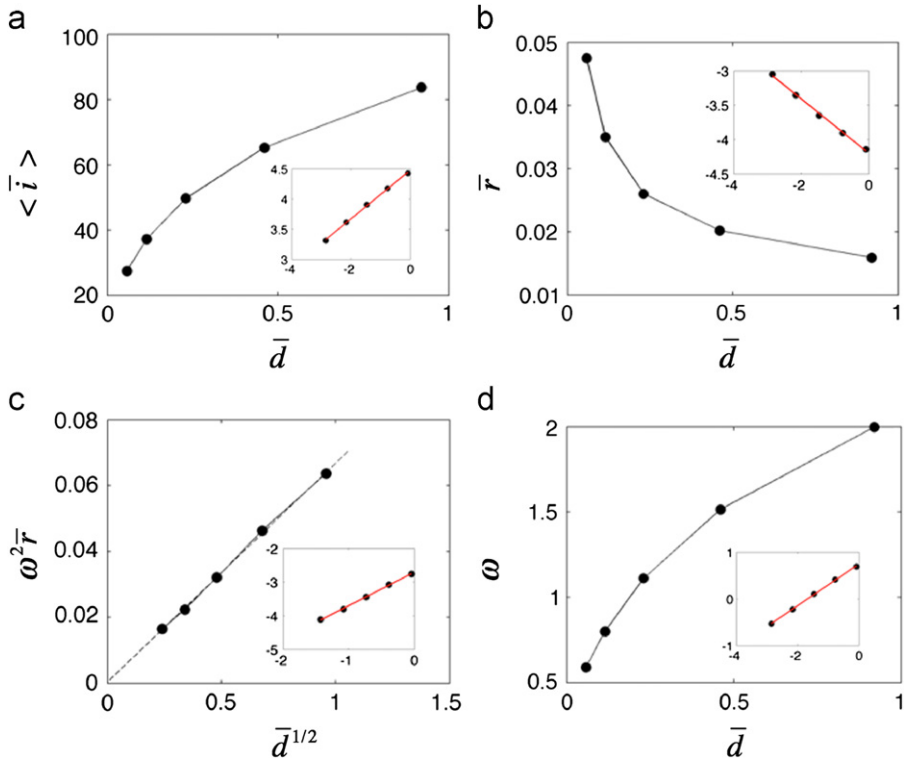

Fig. 2. *Simulations*: effects of rotation rate on mean current, required resistance, and frequency for oscillations that occur close to Hopf bifurcation point at fixed Hopf potential $\bar{e}_H = 35.448$ with $\epsilon = 1$. (a) Nearly square root dependence of mean current on rotation rate. Inset: ln–ln plot giving slope 0.40; (b) nearly inverse square root dependence of required resistance on rotation rate. Inset: ln–ln plot giving slope -0.39; (c) theoretically predicted linear relationship between $\omega^2\bar{r}$ and $\bar{d}^{0.5}$. Dashed line: linear fit. Inset: ln–ln plot giving slope 0.99; and (d) square root dependence of frequency on rotation rate. Inset: ln–ln plot giving slope 0.45.

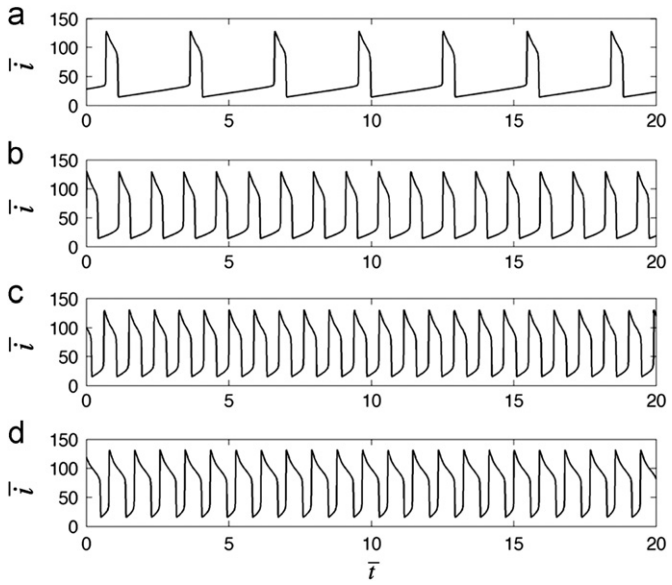

Fig. 3. *Simulations*: relaxation current oscillations at different rotation rates at $\bar{r} = 0.02$, $\epsilon = 0.1$, and $\bar{v} = 37.000$. (a) $\bar{d} = 0.2$; (b) $\bar{d} = 0.4$; (c) $\bar{d} = 0.6$; and (d) $\bar{d} = 0.8$.

quickly disappear and the dynamics is restricted to the $\bar{e}$ nullcline where $d\bar{e}/d\bar{t} = 0$ in Eq. (13)

$$\bar{c} = \frac{\bar{v} - \bar{e}}{120\bar{r}\bar{k}(\bar{e})} \tag{17}$$

The nullcline is represented in the $\bar{e}$ *vs.* $\bar{c}$ relationship in Fig. 4c and d. Note that the $\bar{e}$ nullcline does not depend on rotation rate. For comparison, the $\bar{c}$ nullclines, where $d\bar{c}/d\bar{t} = 0$ in Eq. (14) is also plotted in the figure

$$\bar{c} = \frac{1}{1 + (15\bar{k}(\bar{e})/16\sqrt{\bar{d}})} \tag{18}$$

The $\bar{c}$ nullcline exhibits strong dependence on the rotation rate.

The oscillations take place along the stable branches (with negative slope) of the $\bar{e}$ nullcline as shown in Fig. 4d. For example, starting from point A, the system moves along the nullcline to point B, where the stable branch of the $\bar{e}$ nullcline ends and thus a quick jump to point C occurs; after this transition the system slowly tracks the $\bar{e}$ nullcline again up to point D where a quick jump occurs to point A and the cycle restarts. (Similar nullcline analysis of electrochemical oscillations has been performed to interpret the existence of bistability and oscillations (Koper, 1996; Krischer, 1999; Toni et al., 1998)).

According to Eq. (17), the $\bar{e}$ nullcline is independent of the rotation rate. This is demonstrated in Fig. 4c where the nullclines are shown as function of the rotation rate. The $\bar{c}$ nullcline, however, exhibits strong dependence on the rotation rate. The position of the $\bar{c}$ nullcline simply determines the velocity at which the phase points rotate around the limit cycle; this velocity depends on the rotation rate. Because of the independence of the fast variable $\bar{e}$ nullcline on the rotation rate, no change of maximum/minimum/transition points in the oscillation waveform is observed.

We thus see that for relaxation oscillators, the model equations predict that as the rotation rate changes, the amplitude (and the transition points) will remain constant at constant circuit potential. This invariance is strong indication that the rotation rate parameter does not occur in the dynamical equation of the fast variable, in our example, the electrode potential.

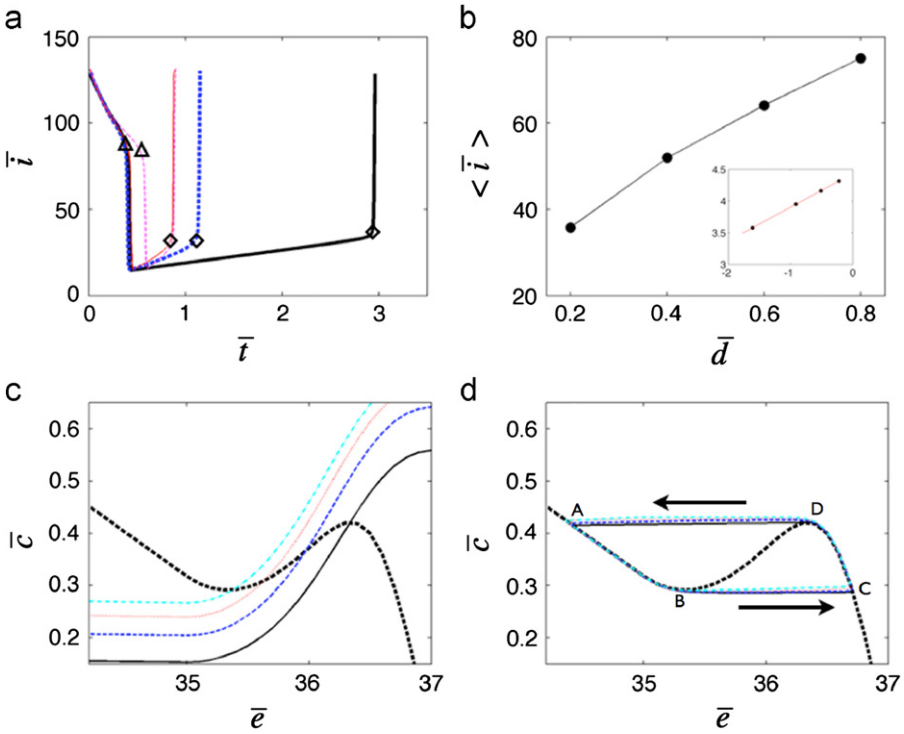

Fig. 4. *Simulations*: changes of characteristics of relaxation oscillations with increase in rotation rate. (a) Oscillation waveforms at different rotation rates. Thick solid line: $\bar{d}=0.2$. Thick dashed line: $\bar{d}=0.4$. Thin solid line: $\bar{d}=0.6$. Thin dashed line: $\bar{d}=0.8$. The triangle and diamond symbols indicate the upper and lower transitions for the waveforms; (b) square root dependence of mean current on rotation rate. Inset: ln–ln plot giving slope 0.53; (c) nullclines for fast variable electrode potential $\bar{e}$ (thick dashed line) for slow variable $\bar{c}$ (thin lines). For $\bar{c}$ nullcline from bottom to top: $\bar{d}=0.2$ (solid), $\bar{d}=0.4$ (dashed), $\bar{d}=0.6$ (dotted), $\bar{d}=0.8$ (dash–dot); and (d) the $\bar{e}$ nullcline (thick dashed line) and the oscillations at different rotation rates ($\bar{d}=0.2$: solid line, $\bar{d}=0.4$: dashed line; $\bar{d}=0.6$: dotted line; $\bar{d}=0.8$: dash–dot line) in the $\bar{e}$–$\bar{c}$ plane. Model parameters are same as in Fig. 3. Letters A, B, C, and D denote nullcline transition points that define the waveform of oscillations.

3.2. Experimental results

We have performed a series of experiments with Cu electrodissolution to confirm the effect of rotation rate on frequency of oscillation (close to Hopf bifurcation) and waveform (for relaxation oscillators).

3.2.1. Effect of rotation rate on oscillation frequency for oscillations close to Hopf bifurcation

Fig. 5a shows current oscillations just above a Hopf bifurcation (by about 5 mV) in the experiment with a frequency of $\omega=2.545$ Hz at $V=201$ mV, $d=1000$ rpm, and $R=77\,\Omega$. From the mean current of the oscillations ($\langle i\rangle=4.293$ mA) we can approximate the Hopf potential as $e_H=V-\langle i\rangle R=-130$ mV.

It is possible to approximate the frequency of the oscillations using the frequency formula (Eqs. (3) and (5)) and the chronoamperometric potential step described in Section 3.1.2. We have measured the double layer capacitance of the electrode at open circuit potential with impedance spectroscopy (Bard and Faulkner, 1980) and obtained $C_dA=30\,\mu$F. In Fig. 5a $R=77\,\Omega$, therefore, $\tau_{el}=C_dAR=2.31$ ms. In a chronoamperometric potential step experiment shown in Fig. 5b and c we can approximate the chemical timescale. The potential step was accomplished (without added external resistance in the cell) to a value of circuit potential where $e=-130$ mV; this value corresponds to that of e_H in the oscillatory region. Linear fit to the semilogarithmic plot of the exponentially decaying current (Fig. 5c) gives a slope of -0.85 1/s, i.e., $\tau_{chem}=1/0.85$, $s=1.18$ s. The frequency thus can be calculated with Eq. (5) as $\omega=3.05$ Hz. This is an excellent approximation of the experimental frequency of 2.545 Hz. The formula overestimates the frequency because it gives only an upper bound. Note that similar to the numerical simulation in Section 3.1.2, we can estimate the ratio of electrical and chemical timescales: $\tau_{el}/\tau_{chem}=2.0\times10^{-3}$. This small parameter is one order of magnitude smaller than that obtained in numerical simulation (0.0326).

Next we test the effect of rotation rate on the frequency. Experiments were performed for rotation rate range 700–1400 rpm. For each rotation rate, the resistance and circuit potential was adjusted in such a way that at the Hopf bifurcation point the electrode potential was $e_H=-48\pm0.5$ mV and the mean current and the frequency of the oscillations were recorded. As it is shown in Fig. 6, the mean current exhibits nearly square root dependence ($\langle i\rangle\propto d^{0.59}$) and the resistance needed for oscillations decreases with increasing the rotation rate close to the expected inverse square root dependency $R\propto d^{-0.45}$. The ω^2R quantity exhibits linear dependence on $\sqrt{d}$ and the dependence of frequency on rotation rate is very close to the expected square root equation ($\omega\propto d^{0.47}$).

The experiments thus confirm that the frequency of the oscillations, under the constraint of constant Hopf potential and close to the Hopf bifurcation point, exhibits square root dependence on rotation rate in Cu electrodissolution.

3.2.2. Effect of rotation rate on oscillation waveform for relaxation oscillators

The Cu electrodissolution system also exhibits relaxation type oscillations at large series resistance R and at circuit potentials further away from the Hopf bifurcation points. Relaxation oscillations are shown in Fig. 7 for rotation rates $d=1300$, 1400, 1500, and 1600 rpm. At the applied circuit potential (200 mV) oscillations do not occur below 1300 rpm and above 1600 rpm. (Note that in contrast to oscillations in the Hopf region, we compare the behavior at fixed circuit potential instead of the Hopf potential.)

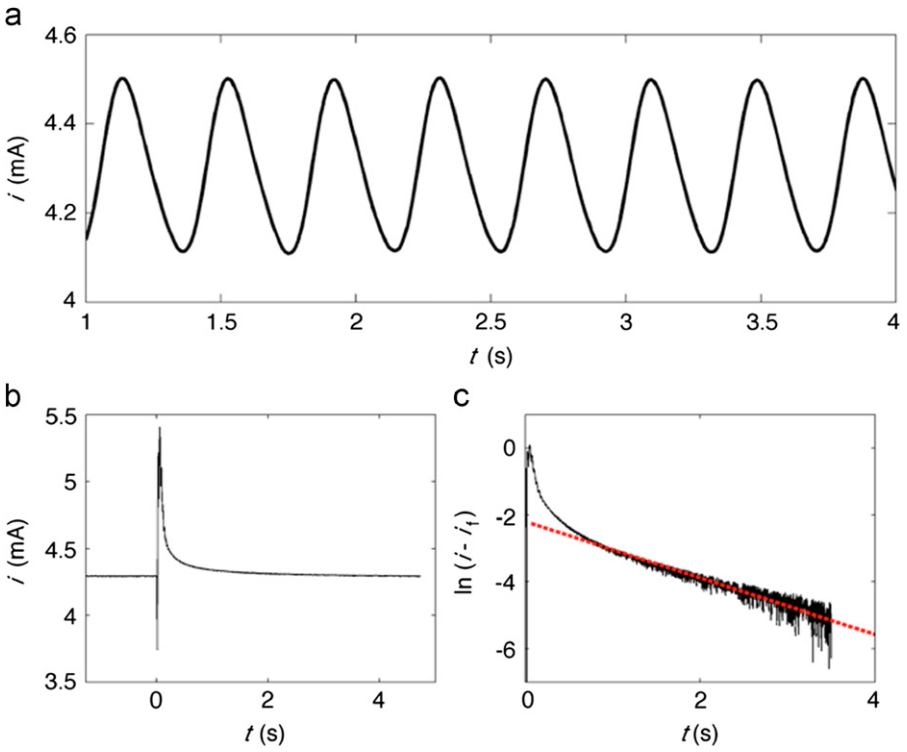

Fig. 5. *Experiments*: smooth periodic current oscillations close to Hopf bifurcation (top) and determination of chemical time-scale using step chronoamperometry (bottom) in copper electrodissolution at rotation rate $d=1000$ rpm and $T=10$ °C. (a) Time series of current oscillations with frequency of $\omega=2.545$ Hz, $R=77\ \Omega$, $V=201$ mV; (b) potential step response with small series resistance ($R=17\ \Omega$). At $t=0$ the circuit potential was changed from $V=-28.5$ to -54 mV; the latter corresponds to the same Hopf potential ($e_H=-130$ mV) as shown in panel b. The final current $i_f=4.29$ mA; and (c) semilogarithmic plot for the exponential decay shown in panel b. The slope of the fitted dashed line is -0.85 1/s.

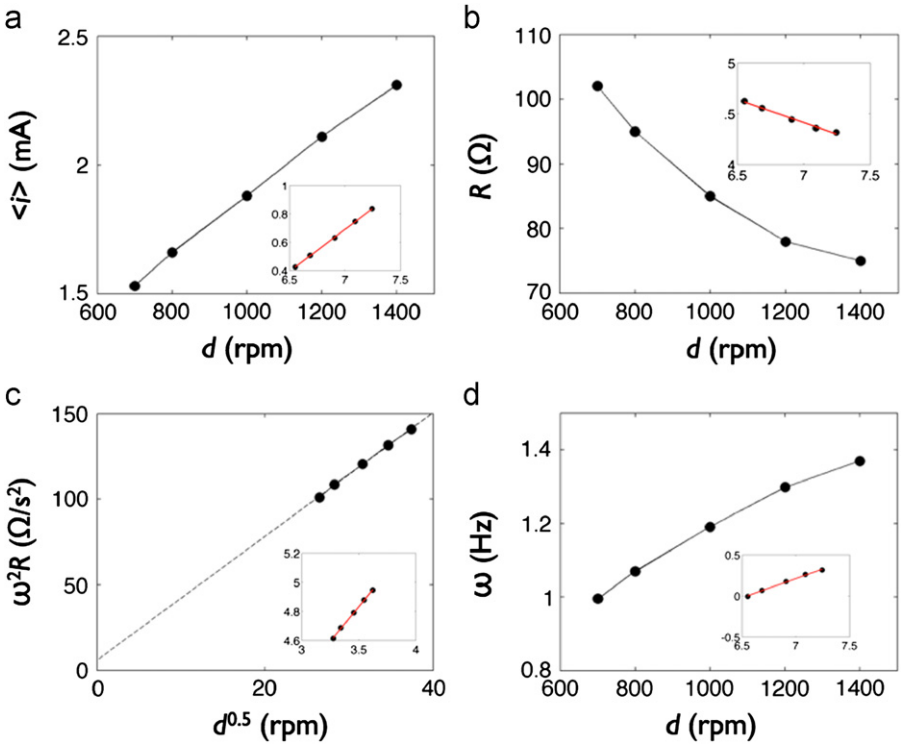

Fig. 6. *Experiments*: effects of rotation rate on mean current, required resistance, and frequency for oscillations that occur close to Hopf bifurcation point at fixed Hopf potential $e_H=-48$ mV $\pm$ 0.5 mV. $T=-5$ °C. (a) Nearly square root dependence of mean current on rotation rate. Inset: ln–ln plot giving slope 0.59; (b) nearly inverse square root dependence of required resistance on rotation rate. Inset: ln–ln plot giving slope -0.45; (c) theoretically predicted linear relationship between ω^2R and $d^{0.5}$. Dashed line: linear fit. Inset: ln–ln plot giving slope 0.95; and (d) square root dependence of frequency on rotation rate. Inset: ln–ln plot giving slope 0.47.

The oscillation waveforms are characterized by low and high current states (where the variations are slow) and quick transitions (jumps) between them. Careful inspection of the waveforms in Fig. 8a indicates that similar to the numerical findings the maxima, minima, and the two transition points of the oscillations do not depend on the rotation rate. The mean current, however, increases with increase of rotation rate and follows the Levich equation as $\langle i \rangle \propto d^{0.59}$. The mean current level increase is established by keeping the maxima, minima, and the transition points of the oscillations at constant level: at low rotation rate (Fig. 7a), the current stays in the low current state for longer period while at large rotation rate (Fig. 7d) the current stays in the higher current state for longer period.

As it was pointed out in Section 3.1.3, the independence of the oscillation minima and maxima and the transition points with rotation rate is an indication that rotation rate does not affect the nullcline structure of the fast variable. The relatively simple experimental test with effect of rotation rate on waveform of relaxation oscillators thus could help elucidate the structure of the ordinary differential equations governing dynamical behavior of the electrochemical oscillatory system.

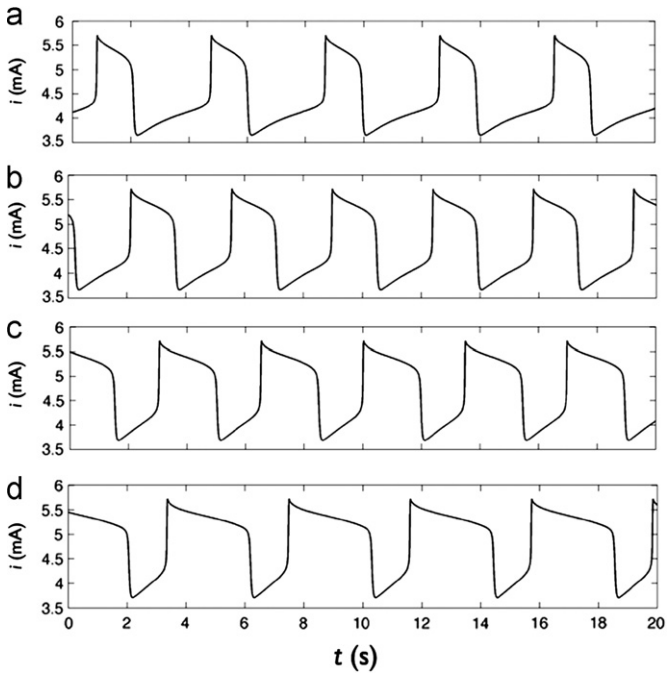

Fig. 7. *Experiments*: relaxation current oscillations at different rotation rates at $R=150\,\Omega$ and $V=0.200$ V. (a) $d=1300$ rpm; (b) $d=1400$ rpm; (c) $d=1500$ rpm; and (d) $d=1600$ rpm. $T=5$ °C.

4. Discussion

The dynamical features of an electrochemical oscillatory system, Cu dissolution in phosphoric acid was investigated in two parameter regions that gave rise to smooth oscillations close to Hopf bifurcation and relaxation oscillations.

Close to Hopf-bifurcation, we showed by theoretical analysis, numerical simulations, and experiments that the frequency increases with rotation rate, and an approximate square root relationship $\omega \propto \sqrt{d}$ was observed. The results further confirm the applicability of the frequency formula (Kiss et al., 2009b) and various scaling relationships (Kiss et al., 2009a) that govern the dynamical features of negative differential resistance electrochemical oscillators.

We have developed a simple potential step chrohoamperometric technique with which the chemical time-scale of the electrochemical reaction system can be determined for the oscillatory behavior. This time-scale was shown to be accurate in predicting the approximate frequency of the oscillations provided that the electrical time-scale is known. A simple experiment in the non-oscillatory region thus have predictive power on dynamical features of oscillatory reaction. The experiments also further confirm the benefits of studying the dynamical features of electrochemical oscillatory systems close to Hopf bifurcation studied under the same electrode potential instead of the more common circuit potential. The presented scaling laws are recovered only under the same Hopf potential which eliminates the potential dependence of electrochemical rate constant.

In parameter region where relaxation oscillations occur, we found that the waveform properties (maximum, minimum, and transition points) did not depend on rotation rate. Our analysis indicated that the rotation rate did not affect the nullcline of the fast variable (electrode potential) in the system; because oscillations take place on the stable branches of the nullclines, the shape of the limit-cycle in the state space does not change with rotation rate. Although nullcline analysis has been a common technique for analysis of chemical (Scott, 1994) and electrochemical (Koper, 1996; Krischer, 1999; Toni et al., 1998) oscillators, usually the technique is used for interpretation of number/stability of steady-states and existence of limit cycles. Our results indicate that the

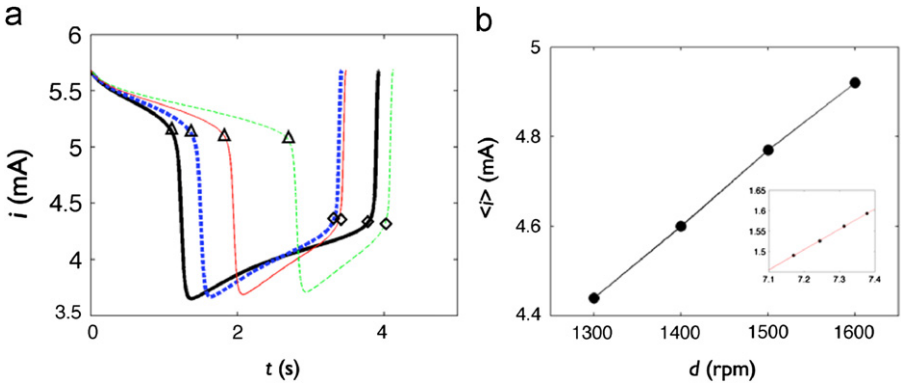

Fig. 8. *Experiments*: changes of characteristics of relaxation oscillations with increase in rotation rate. (a) Oscillation waveforms at different rotation rates: thick solid line: $d=1300$ rpm; thick dashed line: $d=1400$ rpm; thin solid line: $d=1500$ rpm; and thin dashed line: $d=1600$ rpm. The triangle and diamond symbols indicate the upper and lower transitions for the waveforms and (b) square root dependence of mean current on rotation rate. Inset: ln–ln plot giving slope 0.50. (Experimental conditions are the same as in Fig. 7.)

analysis of the shape of relaxation oscillators could be a simple technique to explore the mathematical structure of the governing ordinary differential equations, e.g., finding out the dependency of ordinary differential equation of the fast variable on parameters. In the studied electrochemical model, similar invariant properties would be expected for the effect on waveform of bulk concentrations (c_0) and diffusion coefficients (D) of electroactive species. At the present stage of the theory of electrochemical oscillations (Koper, 1996; Krischer, 1999), this information perhaps seems trivial, however, for novel oscillatory systems parametric studies on waveform of relaxation oscillators could provide decisive experimental data for differentiating suitable oscillatory mechanisms.

In classical electrochemical systems related to steady states of stable electrochemical cells, the Levich equation (Bard and Faulkner, 1980) is applied the describe the mass-transport limited current which is proportional to the square root of rotation rates, $i \propto \sqrt{d}$. In our experiments with smooth and relaxation oscillation, we have approximately recovered this equation for the mean current of the oscillations. Because in the experiments, the oscillations occur close to the mass-transfer limited region, the relationship is not unexpected for the smooth oscillations that have small, harmonic waveform. However, for the large amplitude current oscillations in the relaxation region we also confirmed the dependency, which cannot be easily interpreted, especially, considering that the amplitude of the oscillation remains constant. With the smooth oscillators close to the Hopf bifurcation we found that not only the mean current, but the frequency as well scales with the square root of the rotation rate $\omega \propto \sqrt{d}$. We note that this square root dependence is not a direct consequence of the Levich equation but comes from the unique role of the mass transfer mechanism in the generation of electrochemical oscillations.

We have tested the prediction of a simple negative differential resistance model using Cu dissolution system. The generality of the findings are thus constrained by the quite simple dynamical features of the model. Nonetheless, there are other experimental systems where Eqs. (1) and (2) can describe the dynamics; this includes reduction of cations and anions (Koper, 1996; Koper and Sluyters, 1993b), e.g., indium(III) reduction in the presence of thiocyanate. Many electrochemical models need (at least) three variables to describe the dynamics; for example, in iron electrodissolution surface hydrogen and metal ion concentrations should be considered in addition to the electrode potential (Koper and Sluyters, 1993a; Organ et al., 2003). The test of the model predictions could be a particular challenge in this system. In many electrochemical systems the negative differential resistance is hidden (Koper, 1996; Koper and Sluyters, 1994; Krischer, 1999); in these examples the frequency formula should be modified (Kiss et al., 2009b) and thus further work is required to predict rotation rate dependencies.

We have utilized two major simplifying concepts that were found to have predictive power for decoding the dynamical features of the electrochemical system. First, we investigated the behavior of the system only close to Hopf bifurcation point. This application of the principle of critical simplification (Yablonsky et al., 2003) allowed us to study the frequency of the oscillations in a simple manner. The frequency of the oscillation is defined by time-scales of the system, therefore, the study gave information on how the different electrical and chemical time-scales interact to produce the value of the frequency. In previous example, PCS was applied to saddle-node bifurcation to describe the rate of the reaction. (Yablonsky et al., 2003) Because in electrochemical systems saddle-node bifurcations are also common (Koper, 1996; Krischer, 1999) and detailed information have been reported for various systems (Jurczakowski and Orlik, 2007; Koper et al., 1992; Lev et al., 1989; Malkhandi et al., 2009), it is likely the PCS has wider application in electrochemical, and possibly in other chemical systems as well. The second simplifying technique that we applied for relaxation oscillators was the nullcline technique. A powerful expansion of the nullcline technique utilizes manifolds (Gorban and Karlin, 2005) that represent slow, strongly interdependent variation of variables. Extensive use of the manifolds approach could greatly enhance decoding the dynamics of chemical complexity in various experimental systems; our work is a step toward such experimental application. To take advantage of different manifold theories, the concurrent measurement of many chemical species would be required for the system. In traditional electrochemical experiments the currents are measured, however, in the past two decades significant progress has been made in measuring surface coverages/concentrations, e.g., with in-situ IR spectroscopy (Morschl et al., 2008; Samjeske and Osawa, 2005) or electrochemical mass spectrometry (Seidel et al., 2010). The widespread application of these experimental techniques along with manifold description of complex system is expected to greatly enhance our understanding of dynamics of chemical reaction processes.

5. Conclusions

The effect of mass-transfer conditions through variations of rotation rate of a disk electrode on the oscillatory dynamics of a negative-differential resistance electrochemical system was studied in numerical simulations and experiments. For oscillations close to Hopf bifurcation the frequency depends approximately on the square root of the rotation rate. The dependency was interpreted in a theoretical framework using bifurcation analysis and the principle of critical simplification. For relaxation oscillations, the amplitude and the transition points between the high and low current states did not depend on the rotation rate. The parametric dependency of waveform of relaxation oscillators can thus be applied to classify system parameters on the their role of the dynamics of the fast subsystem. The results could find applications for the growing field of design of chemical (De Kepper et al., 1981; Kurin-Csörgei et al., 2005, 2006; Lagzi et al., 2010) and biological (Elowitz and Leibler, 2000) oscillators. For example, the frequency of oscillator could be tuned in a predictive manner by changing mass transfer conditions. Batch pH oscillators were recently obtained by optimization of mass transfer conditions using a layer of silica gel (Poros et al., 2011). Relaxation oscillators could be good candidates for design of oscillations whose amplitude should not depend on parameters that do not affect the dynamics of the fast subsystem. Biological oscillations can be designed with genetic circuits. (Danino et al., 2010; Elowitz and Leibler, 2000) Mass transfer between the cytosol, cell nucleus, and intercellular media could affect the oscillator properties (Danino et al., 2010; Leloup, 2004); the exploration of the mass transfer affects in biological oscillator system, with techniques similar to those applied in our study, could aid the design of biological oscillators with proper amplitude and frequency characteristics.

Acknowledgments

This material is based upon work supported by the National Science Foundation under Grant no. CHE-0955555. Acknowledgment is made to the Donors of the American Chemical Society Petroleum Research Fund for support of this research. The work by GV was supported by the Hungarian OTKA Grant 81646 and by the TÁMOP 4.2.1./B-09/1/KONV-2010-0007 project. The project is implemented through the New Hungary Development Plan, co-

financed by the European Social Fund and the European Regional Development Fund.

References

Albahadily, F.N., Ringland, J., Schell, M., 1989. Mixed-mode oscillations in an electrochemical system. I. A Farey sequence which does not occur on a torus. J. Chem. Phys. 90, 813–821.

Albahadily, F.N., Schell, M., 1988. An experimental investigation of periodic and chaotic electrochemical oscillations in the anodic-dissolution of copper in phosphoric-acid. J. Chem. Phys. 88, 4312–4319.

Bard, A.J., Faulkner, L.R., 1980. Electrochemical Methods. Wiley, New York.

Bindal, A., Ierapetritou, M.G., Balakrishnan, S., Armaou, A., Makeev, A.G., Kevrekidis, I.G., 2006. Equation-free, coarse-grained computational optimization using timesteppers. Chem. Eng. Sci. 61, 779–793.

Boovaragavan, V., Methakar, R.N., Ramadesigan, V., Subramanian, V.R., 2009. A mathematical model of the lead-acid battery to address the effect of corrosion. J. Electrochem. Soc. 156, A854–A862.

Bykov, V., Gol'dhstein, V., Maas, U., 2008. Simple global reduction technique based on decomposition approach. Combust. Theory Modelling. 12, 389–405.

Danino, T., Mondragon-Palomino, O., Tsimring, L., Hasty, J., 2010. A synchronized quorum of genetic clocks. Nature 463, 326–330.

De Kepper, P., Epstein, I.R., Kustin, K., 1981. A systematically designed homogeneous oscillating reaction: The arsenite–iodate–chlorite system. J. Am. Chem. Soc. 103, 2133–2134.

Elowitz, M.B., Leibler, S., 2000. A synthetic oscillatory network of transcriptional regulators. Nature 403, 335–338.

Epstein, I.R., Pojman, J.A., 1998. An Introduction to Nonlinear Chemical Dynamics: Oscillations, Waves, Patterns, and Chaos. Oxford University Press, Oxford.

Ermentrout, B., 2002. Simulating, Analyzing, and Animating Dynamical Systems: A Guide to XPPAUT for Researchers and Students. SIAM, Philadelphia.

Gáspár, V., Showalter, K., Peng, B., 1991. False bifurcations in chemical systems: Canards. Philos. Trans. R. Soc. London. A 337, 275–289.

Glarum, S.H., Marshall, J.H., 1985. Anodic dissolution of copper into phosphoric acid. I. Voltammetric and oscillatory behavior. J. Electrochem. Soc. 132, 2872–2878.

Gorban, A.N., Karlin, I.V., 2003. Method of invariant manifold for chemical kinetics. Chem. Eng. Sci., 4751–4768.

Gorban, A.N., Karlin, I.V., 2005. Invariant Manifolds for Physical and Chemical Kinetics. Springer-Verlag, Berlin.

Gorban, A.N., Kazantzis, N.K., Kevrekidis, I.G., Öttinger, H.C., Theodoropoulos, C., 2007. Model Reduction and Coarse-Graining Approaches for Multiscale Phenomena. Springer, New York.

Hudson, J.L., Tsotsis, T.T., 1994. Electrochemical reaction dynamics—a review. Chem. Eng. Sci. 49, 1493–1572.

Jurczakowski, R., Orlik, M., 2007. Experimental and theoretical impedance studies of oscillations and bistability in the Ni(II)-SCN-electroreduction at the streaming mercury electrode. J. Electroanal. Chem 605, 41–52.

Kevrekidis, I.G., Gear, C.W., Hummer, G., 2004. Equation-free: The computer-aided analysis of complex multiscale systems. AIChE J. 50, 1346–1355.

Kiss, I.Z., Gáspár, V., Nyikos, L., 1998. Stability analysis of the oscillatory electrodissolution of copper with impedance spectroscopy. J. Phys. Chem. A 102, 909–914.

Kiss, I.Z., Gáspár, V., Nyikos, L., Parmananda, P., 1997. Controlling electrochemical chaos in the copper–phosphoric acid system. J. Phys. Chem. A 101, 8668–8674.

Kiss, I.Z., Kazsu, Z., Gáspár, V., 2009a. Scaling relationship for oscillating electrochemical systems: Dependence of phase diagram on electrode size and rotation rate. Phys. Chem. Chem. Phys. 11, 7669–7677.

Kiss, I.Z., Nagy, T., Gáspár, V., 2011. Dynamical instabilities in electrochemical processes. In: Kharton, V.V. (Ed.), Solid State Electrochemistry II: Electrodes, lntcryaces and Ceramic Membranes, Wiley-VCH, Weinheim.

Kiss, I.Z., Pelster, L.N., Wickramasinghe, M., Yablonsky, G.S., 2009b. Frequency of negative differential resistance electrochemical oscillators: Theory and experiments. Phys. Chem. Chem. Phys. 11, 5720–5728.

Koper, M.T.M., 1996. Oscillations and complex dynamical bifurcations in electrochemical systems. Adv. Chem. Phys. 92, 161–298.

Koper, M.T.M., Gaspard, P., 1992. The modeling of mixed-mode and chaotic oscillations in electrochemical systems. J. Chem. Phys. 96, 7797–7813.

Koper, M.T.M., Gaspard, P., Sluyters, J.H., 1992. Mixed-mode oscillations and incomplete homoclinic scenarios to a saddle focus in the indium/thiocyanate electrochemical oscillator. J. Chem. Phys. 97, 8250–8260.

Koper, M.T.M., Sluyters, J.H., 1991. Electrochemical oscillators: Their description through a mathematical model. J. Electroanal. Chem. 303, 73–94.

Koper, M.T.M., Sluyters, J.H., 1993a. A mathematical model for current oscillations at the active–passive transition in metal electrodissolution. J. Electroanal. Chem. 347, 31–48.

Koper, M.T.M., Sluyters, J.H., 1993b. On the mathematical unification of a class of electrochemical oscillators and their design procedures. J. Electroanal. Chem. 352, 51–64.

Koper, M.T.M., Sluyters, J.H., 1994. Instabilities and oscillations in simple models of electrocatalytic surface reactions. J. Electroanal. Chem. 371, 149–159.

Krischer, K., 1999. Principles of temporal and spatial pattern formation in electrochemical systems. In: Conway, B.E., Bockris, O.M., White, R.E. (Eds.), Modern Aspects of Electrochemistry, Kluwer Academic/Plenum Press, New York.

Krischer, K., Varela, H., 2003. Oscillations and other dynamic instabilities. In: Vielstich, W., Lamm, A., Gasteiger, H.A. (Eds.), Handbook of Fuel Cells—Fundamentals, Technology and Applications, John Wiley & Sons, Chichester, pp. 679–701.

Kurin-Csörgei, K., Epstein, I.R., Orban, M., 2006. Periodic pulses of calcium ions in a chemical system. J. Phys. Chem. A 110, 7588–7592.

Kurin-Csörgei, K., Epstein, I.R., Orbán, M., 2005. Systematic design of chemical oscillators using complexation and precipitation equilibria. Nature 433, 139–142.

Lagzi, I., Kowalczyk, B., Wang, D., Grzybowski, B.A., 2010. Nanoparticle oscillations and fronts. Angew. Chem. Int. Ed. 49, 8616–8619.

Leloup, J., 2004. Modeling the mammalian circadian clock: Sensitivity analysis and multiplicity of oscillatory mechanisms. J. Theor. Biol 230, 541–562.

Lev, O., Wolffberg, A., Pismen, L.M., Sheintuch, M., 1989. The structure of complex behavior in anodic nickel dissolution. J. Phys. Chem. 93, 1661–1666.

Levich, V.G., 1962. Physicochemical Hydrodynamics. Prentice Hall, Englewood Cliffs, N. J.

Malkhandi, S., Bonnefont, A., Krischer, K., 2009. Dynamic instabilities during the continuous electro-oxidation of CO on poly- and single crystalline Pt electrodes. Surf. Sci. 603, 1646–1651.

Morschl, R., Bolten, J., Bonnefont, A., Krischer, K., 2008. Pattern formation during CO electrooxidation on thin Pt films studied with spatially resolved infrared absorption spectroscopy. J. Phys. Chem. C 112, 9548–9551.

Newman, J., 1968. Engineering design of electrochemical systems. Ind. Eng. Chem. 60, 12–27.

Newman, J., Thomas-Alyea, K.E., 2004. Electrochemical Systems, 3rded. Wiley-Interscience, Hoboken, NJ.

Organ, L., Kiss, I.Z., Hudson, J.L., 2003. Bursting oscillations during metal electrodissolution: Experiments and model. J. Phys. Chem. B 107, 6648–6659.

Plenge, F., Varela, H., Lubke, A., Krischer, K., 2003. Quantitative modeling of the oscillatory electrooxidation of hydrogen on Pt in the presence of poisons. Z. Phys. Chem. 217, 365–381.

Poros, E., Horváth, V., Kurin-Csörgei, K., Epstein, I.R., Orbán, M., 2011. Generation of pH-oscillations in closed chemical systems: Method and applications. J. Am. Chem. Soc. 133, 7174–7179.

Roussel, M.R., Fraser, S.J., 2001. Invariant manifold methods for metabolic model reduction. Chaos 11, 196–206.

Samjeske, G., Osawa, M., 2005. Current oscillations during formic acid oxidation on a Pt electrode: Insight into the mechanism by time-resolved IR spectroscopy. Angew. Chem. Int. Ed. 44, 5694–5698.

Schell, M., Albahadily, F.N., 1989. Mixed-mode oscillations in an electrochemical system. II. A periodic-chaotic sequence. J. Chem. Phys. 90, 822–828.

Scott, S.K., 1994. Oscillations, Waves, and Chaos in Chemical Kinetics (Oxford Chemistry Primers). Oxford University Press, USA, New York.

Seidel, Y.E., Jusys, Z., Lindstrom, R.W., Stenfeldt, M., Kasemo, B., Krischer, K., 2010. Oscillatory behaviour in galvanostatic formaldehyde oxidation on nanostructured Pt/glassy carbon model electrodes. Chem. Phys. Chem 11, 1405–1415.

Strasser, P., Eiswirth, M., Koper, M.T.M., 1999. Mechanistic classification of electrochemical oscillators—operational experimental strategy. J. Electroanal. Chem. 478, 50–66.

Strogatz, S.H., 2000. Nonlinear Dynamics and Chaos. Westview Press, Cambridge.

Theodoropoulos, C., Qian, Y.H., Kevrekidis, I.G., 2000. Coarse stability and bifurcation analysis using time-steppers: A reaction-diffusion example. Proc. Natl. Acad. Sci. USA 97, 9840–9843.

Toni, B., Parmananda, P., Bulajich, R., Thieffry, D., 1998. Dynamics of a two-dimensional model for electrochemical corrosion using feedback circuit and nullcline analysis. J. Phys. Chem. B 102, 4118–4122.

Yablonsky, G.S., Mareels, I.M.Y., Lazman, M., 2003. The principle of critical simplification in chemical kinetics. Chem. Eng. Sci. 58, 4833–4842.